8600 Series VSM

Measurement Results

B. C. Dodrill

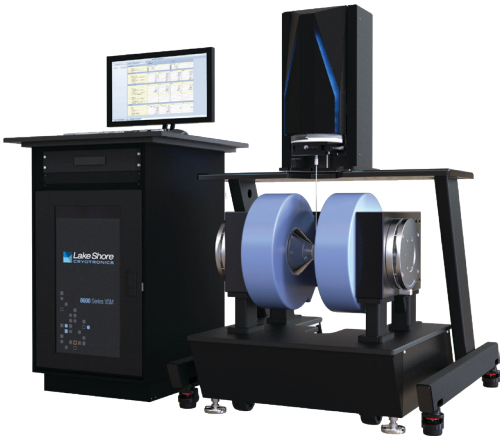

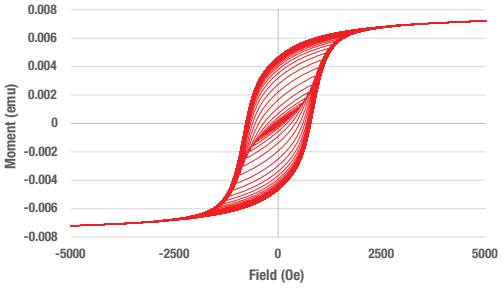

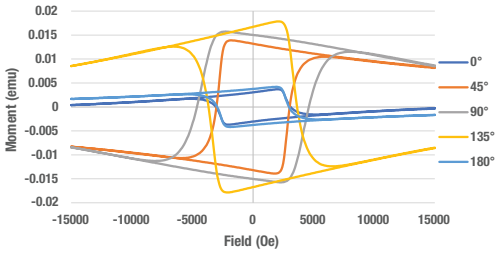

Lake Shore CRYOTRONICS

614.891.2243 | **www.lakeshore.com**

Typical Noise and Low Moment Measurement Results

NOISE AND LOW MOMENT

Figure 1a and 1b

Noise at 100 ms/point (1a) and 10 s/point (1b) averaging. The observed noise is 119.5 nemu and 13 nemu RMS, respectively, consistent with our RMS noise specifications of 150 nemu and 15 nemu, respectively. Measurements are taken with an empty sample holder.

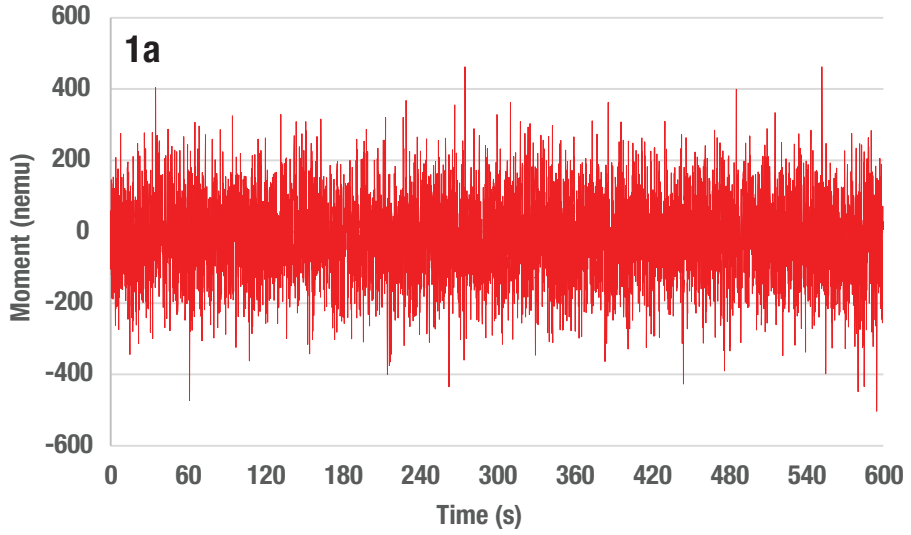

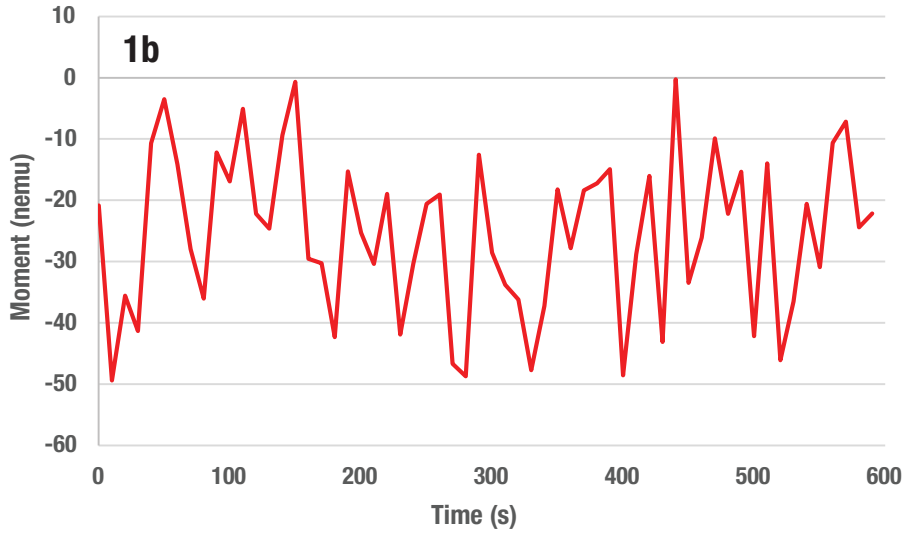

NOISE AND LOW MOMENT

Figure 2

1 min 25 s at 100 ms/point hysteresis loop for a 20 µemu CoPt bit-patterned magnetic media (thin film) sample. The peak-to-peak noise in the data is consistent with the RMS noise specification at 100 ms/point.

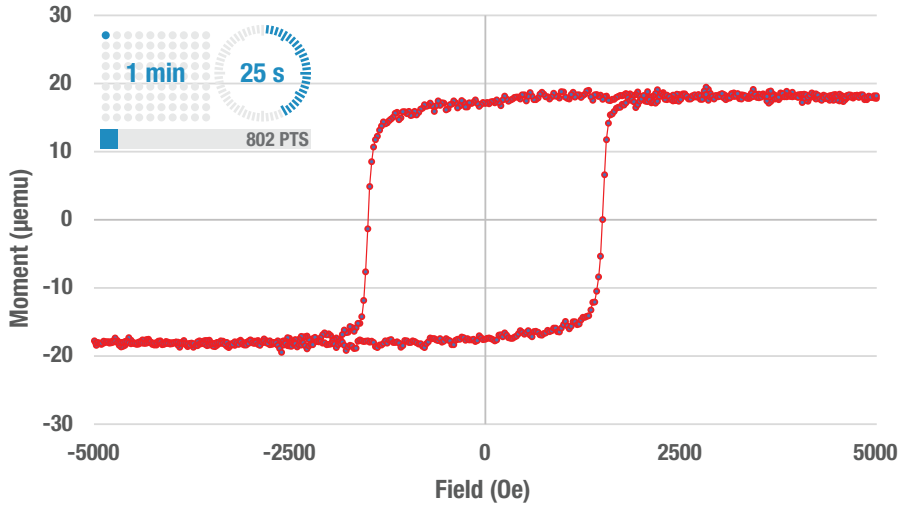

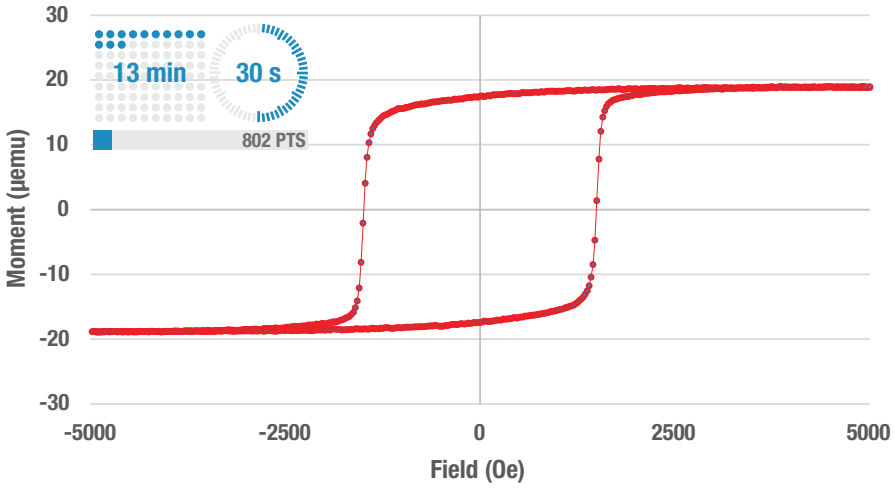

NOISE AND LOW MOMENT

Figure 3

13 min 30 s at 1 s/point hysteresis loop for the 20 µemu CoPt bit-patterned magnetic media (thin film) sample shown in figure 2. The peak-to-peak noise in the data is consistent with the RMS noise specification at 1 s/point. This shows that increasing signal averaging improves signal-to-noise although at the expense of increased measurement time.

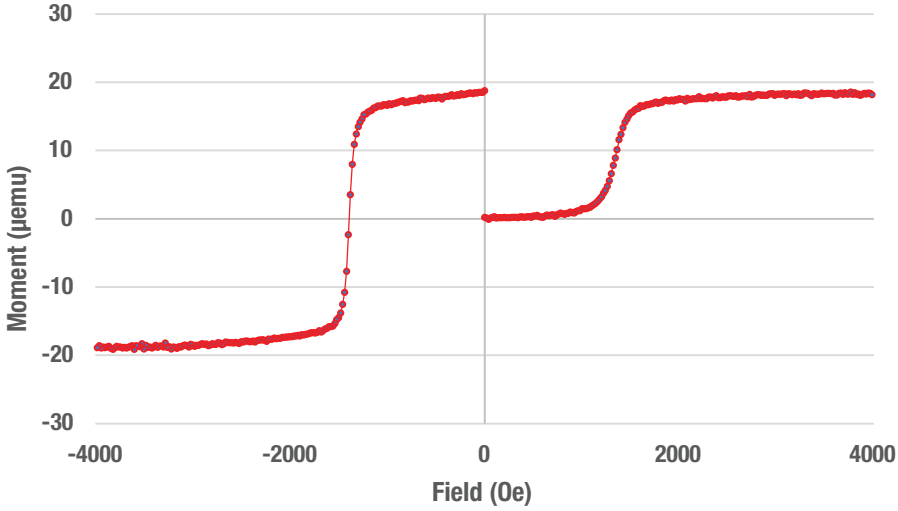

NOISE AND LOW MOMENT

Figure 4

Isothermal (IRM) and DC demagnetization (DCD) remanence curves for the 20 µemu CoPt bit-patterned magnetic media (thin film) sample shown in figures 2 and 3. IRM is measured after the application and removal of a field with the sample initially demagnetized, and DCD is measured from the saturated state by application of increasing demagnetizing fields. Measurement of remanence curves determines only the irreversible component of magnetization and thus enables the phenomena of switching to be deconvoluted from the hysteresis measurement, which generally includes a reversible component.

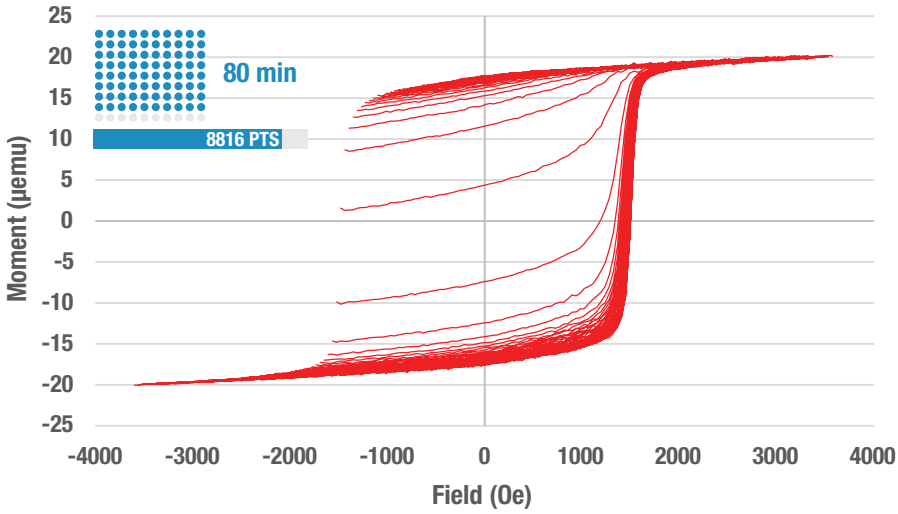

NOISE AND LOW MOMENT

Figure 5

1 h 20 min at 500 ms/point measurement of 100 first-order-reversal-curves (FORCs) for the 20 µemu CoPt bit-patterned magnetic media (thin film) sample shown in figures 2, 3, and 4. FORCs provide information regarding magnetic interactions and coercivity distributions in magnetic materials, information that cannot be obtained from the hysteresis loop alone. In this series of FORCs there are 8,816 points. The fast (1 T/s) field sweep capability of the 8600 together with its high sensitivity makes it possible to record FORCs in a fraction of the time it takes in other magnetometer systems.

NOISE AND LOW MOMENT

Figure 6

10 min 40 s at 1 s/point hysteresis loop for a 20 µemu perpendicular magnetic anisotropy (PMA) thin film. The blue curve is the measured data, which includes a diamagnetic component due to both the sample holder and sample substrate. The orange curve shows background corrected results, which removes the diamagnetic component yielding the hysteresis loop for the film only.

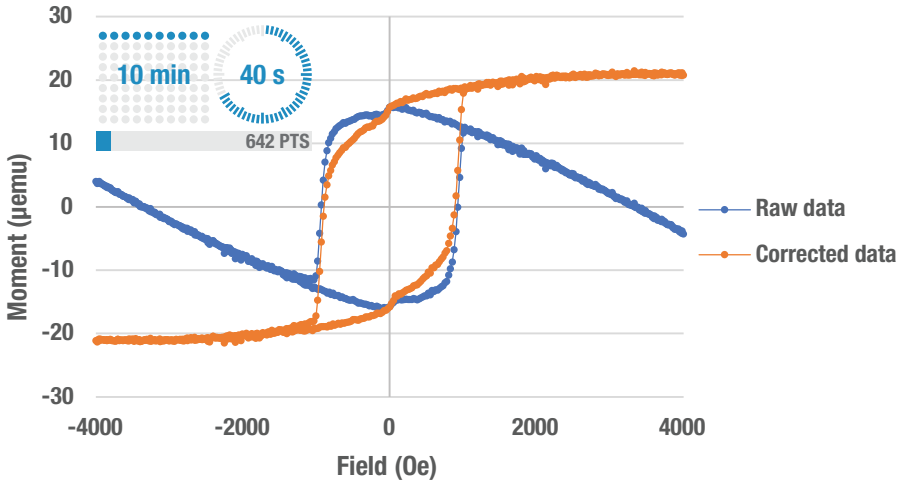

NOISE AND LOW MOMENT

Figure 7

14 min 18 s at 100 ms/point and at 5 mOe field steps for a 40 µemu NiFe (3 nm) thin film. This demonstrates the ability of the 8600 to measure low moment magnetically soft (low coercivity) materials with high precision.

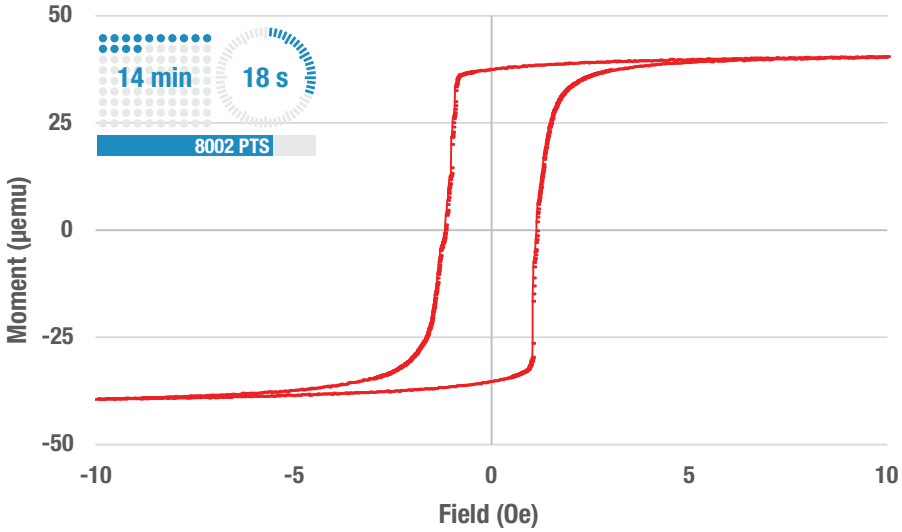

NOISE AND LOW MOMENT

Figure 8

28 min at 2 s/point hysteresis loop for a <2 µemu synthetic antiferromagnetic thin film [Ta (2.5 nm)/ Ru (5 nm)/Co (5 nm)/Ru (0.8 nm)/Co (5 nm)/ Cu (6 nm)/Co (5 nm)/Ru (1.4 nm)/Co (10 nm)/Ta (5 nm)].

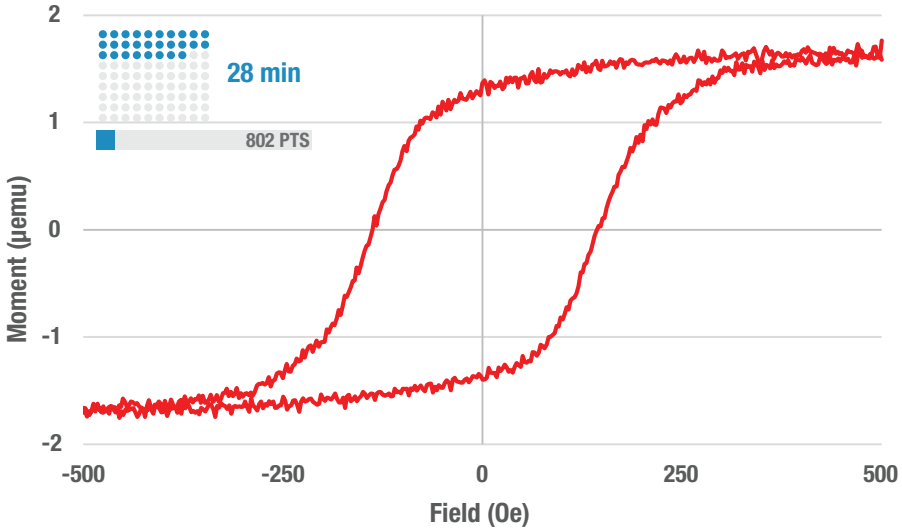

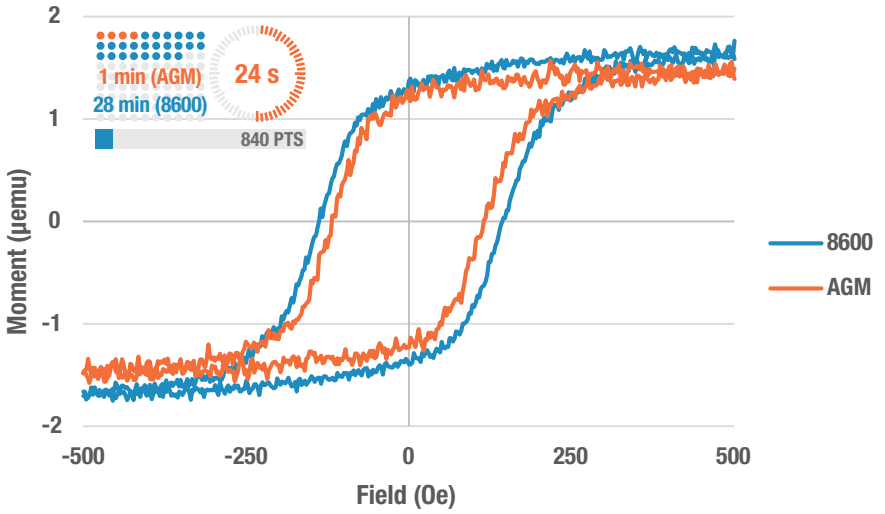

NOISE AND LOW MOMENT

Figure 9

Comparison of 8600 VSM (2 s/point) and AGM (100 ms/point) results for the <2 µemu synthetic antiferromagnetic thin film [Ta (2.5 nm)/ Ru (5 nm)/Co (5 nm)/Ru (0.8 nm)/Co (5 nm)/ Cu (6 nm)/Co (5 nm)/Ru (1.4 nm)/Co (10 nm)/ Ta (5 nm)] shown in figure 8. Note that while the signal-to-noise are comparable in both measurements, the AGM data were recorded in 1/20th the time (1.4 min).

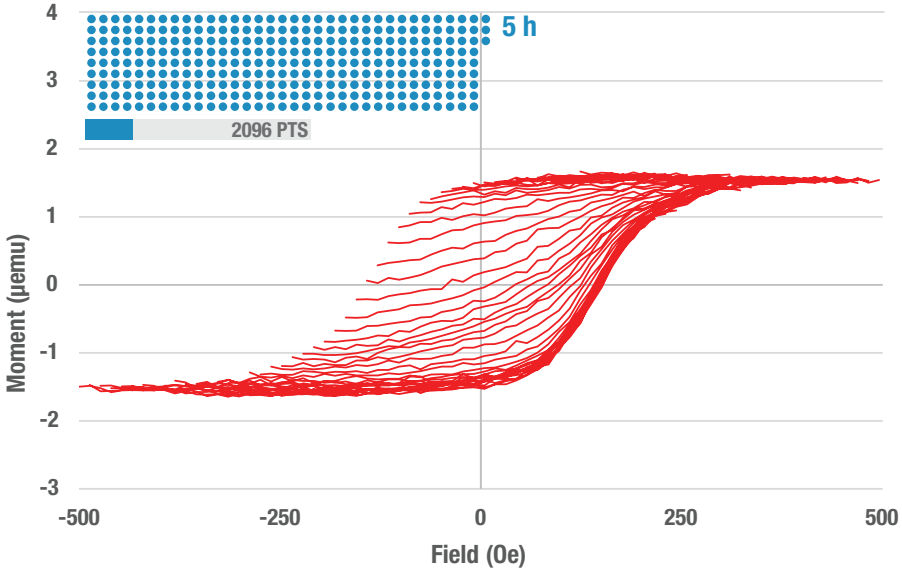

NOISE AND LOW MOMENT

Figure 10

5.5 h at 10 s/point FORC (N = 50) for the <2 µemu synthetic antiferromagnetic thin film [Ta (2.5 nm)/Ru (5 nm)/Co (5 nm)/Ru (0.8 nm)/ Co (5 nm)/Cu (6 nm)/Co (5 nm)/Ru (1.4 nm)/ Co (10 nm)/Ta (5 nm)] shown in figures 8 and 9.

Typical Fast Hysteresis and FORC Measurement Results

FAST HYSTERESIS AND FORC

Figure 1

14 s hysteresis loop measurement
(802 points, 10 ms/point) for a magnetic tape.

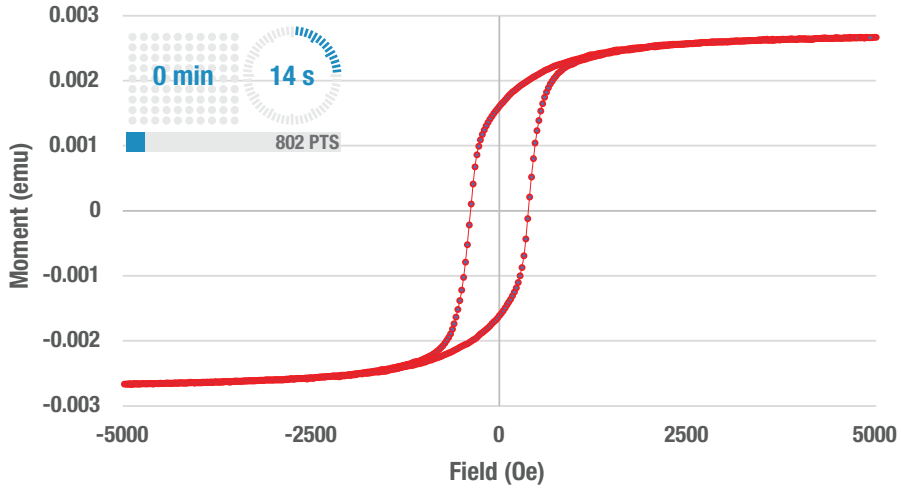

FAST HYSTERESIS AND FORC

Figure 2

26 s hysteresis loop measurement
(2000 points, 10 ms/point) for a bilayer thin film.

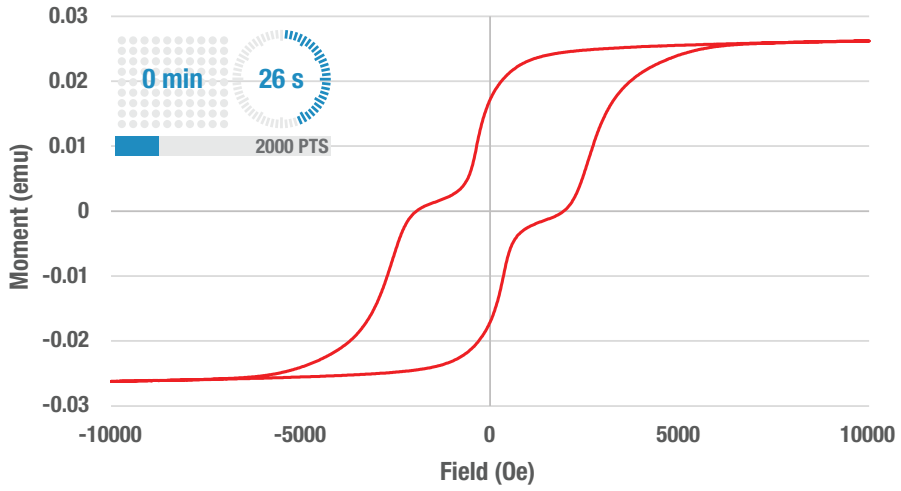

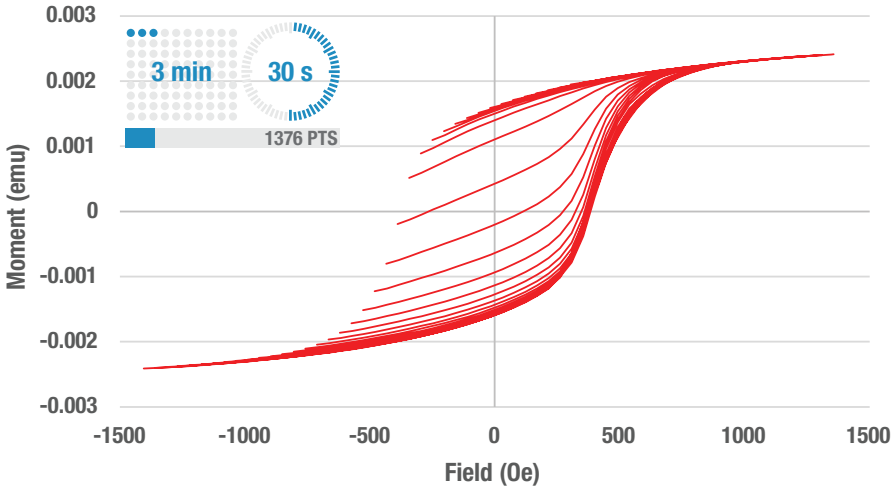

FAST HYSTERESIS AND FORC

Figure 3

3 min 30 s measurement of FORCs (N = 40, 1,376 points, 50 ms/point) for a magnetic tape. The fast (1 T/s) field sweep capability of the 8600 together with its high sensitivity makes it possible to record FORCs in a fraction of the time it takes in other magnetometer systems.

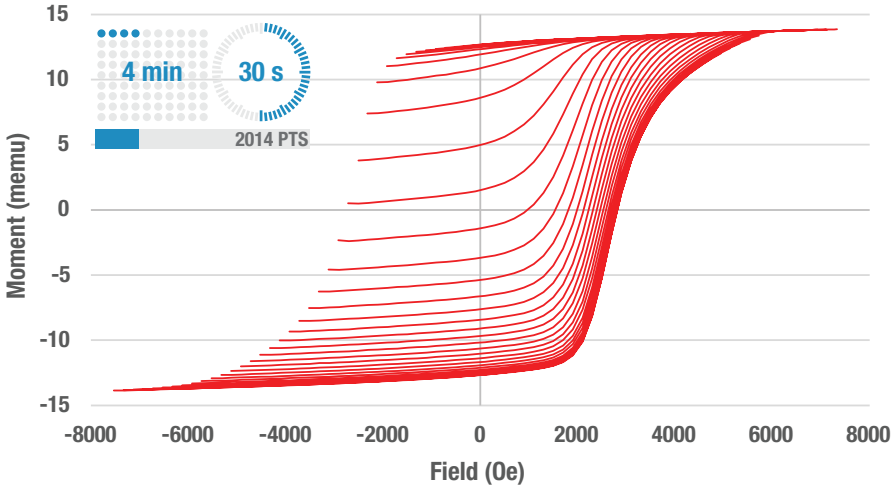

FAST HYSTERESIS AND FORC

Figure 4

4 min 30 s measurement of FORCs (N = 46, 2,014 points, 30 ms/point) for a magnetic stripe. The fast (1 T/s) field sweep capability of the 8600 together with its high sensitivity makes it possible to record FORCs in a fraction of the time it takes in other magnetometer systems.

Typical Low Coercivity Measurement Results

LOW COERCIVITY

Figure 1

Hysteresis loop at 1 mOe steps for a low coercivity Fe microwire. The jumps in the curve are due to Barkhausen noise, which occurs when individual magnetic domains spontaneously flip their magnetization direction.

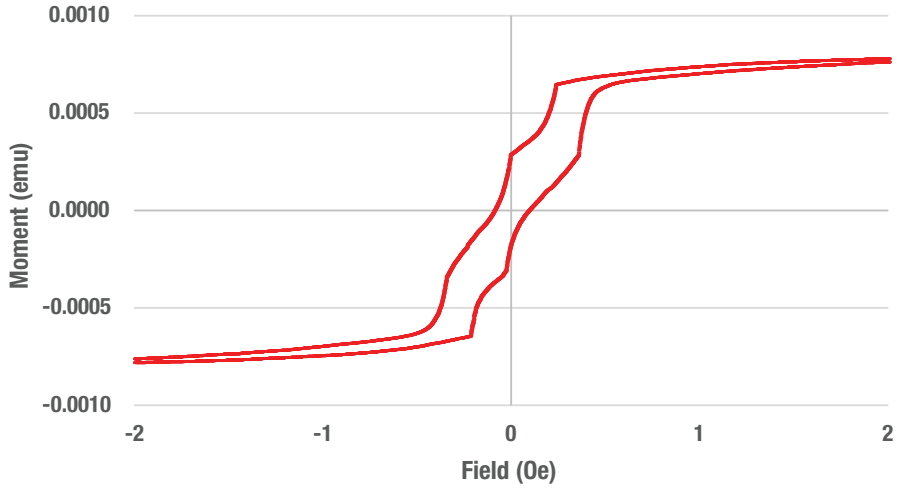

LOW COERCIVITY

Figure 2

Hysteresis loop at 5 mOe steps for a NiFe thin film.

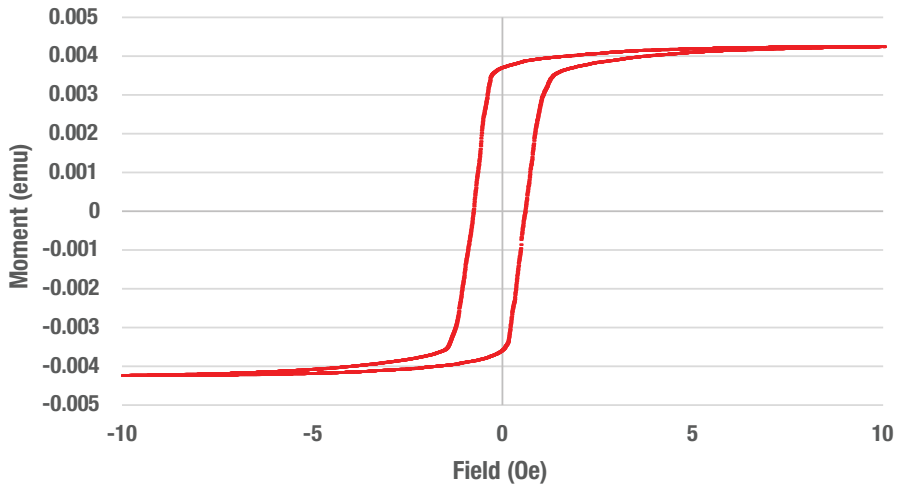

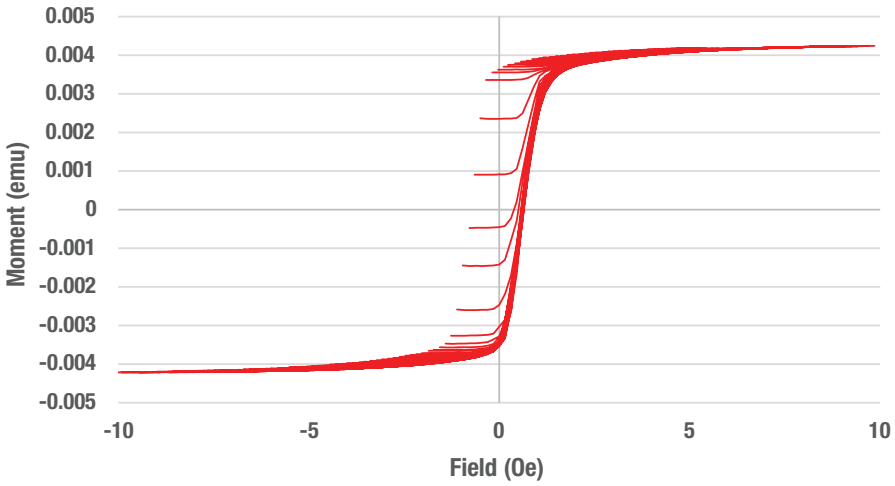

LOW COERCIVITY

Figure 3

FORC (N = 100) for the NiFe thin film shown in figure 2. This shows the ability of the 8600 to measure FORCs on even very low coercivity materials.

Typical Magnetic Multilayer Measurement Results

MAGNETIC MULTILAYER

Figure 1

Hysteresis loops versus angle for a spin-valve stack. When the magnetic field is applied parallel to the exchange bias field the loop is shifted towards the right (positive field values). When applied anti-parallel the loop is shifted towards the left (negative field values). When applied perpendicular the loop is centered at H = 0.

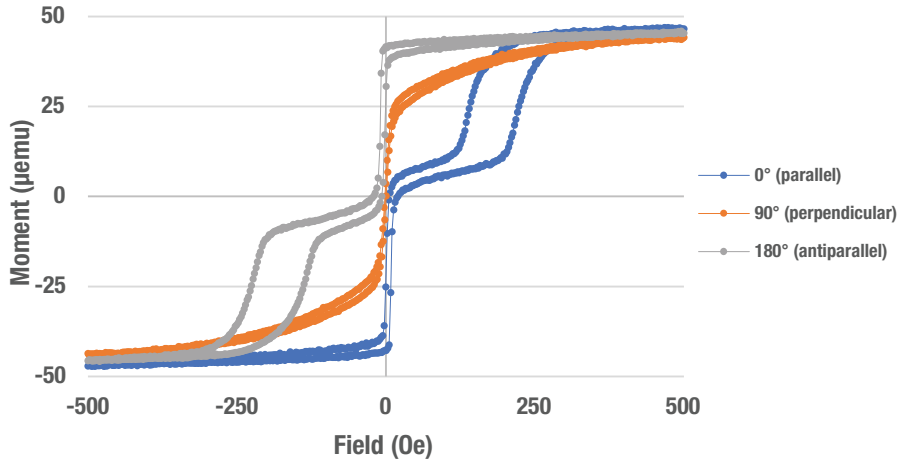

MAGNETIC MULTILAYER

Figure 2

Hysteresis loop for a [FeNi/IrMn] spin-valve. The extra steps in both the descending and ascending branches of the magnetization curve in the 3rd quadrant are related to microstructural defects/roughness of the antiferromagnetic (AFM)/ferromagnetic (FM) interfaces.

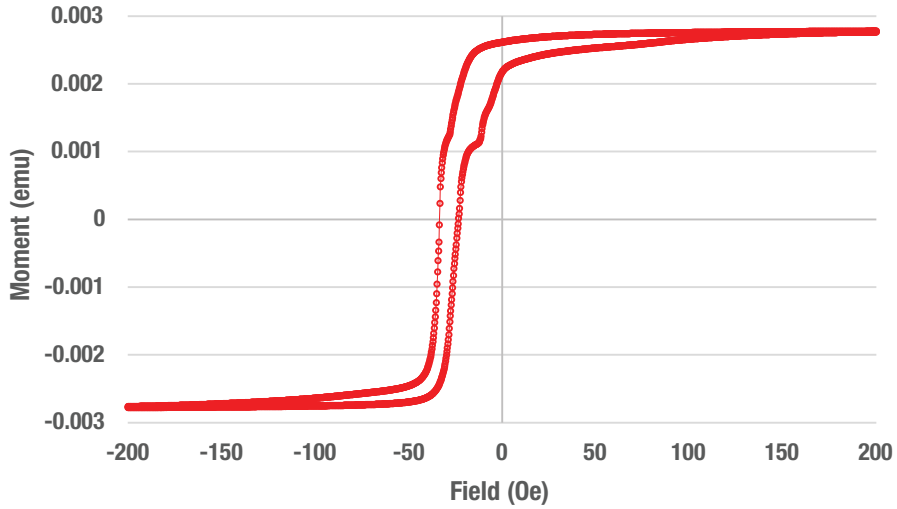

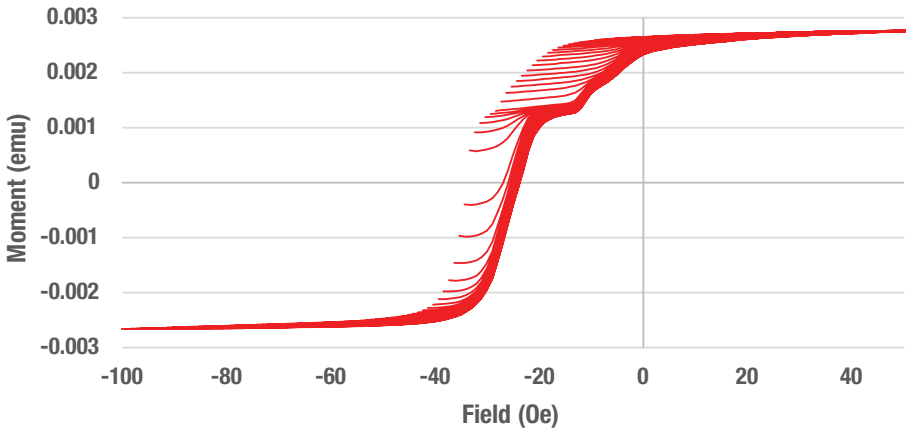

MAGNETIC MULTILAYER

Figure 3

FORC (N = 151) for the [FeNi/IrMn] spin-valve shown in figure 2.

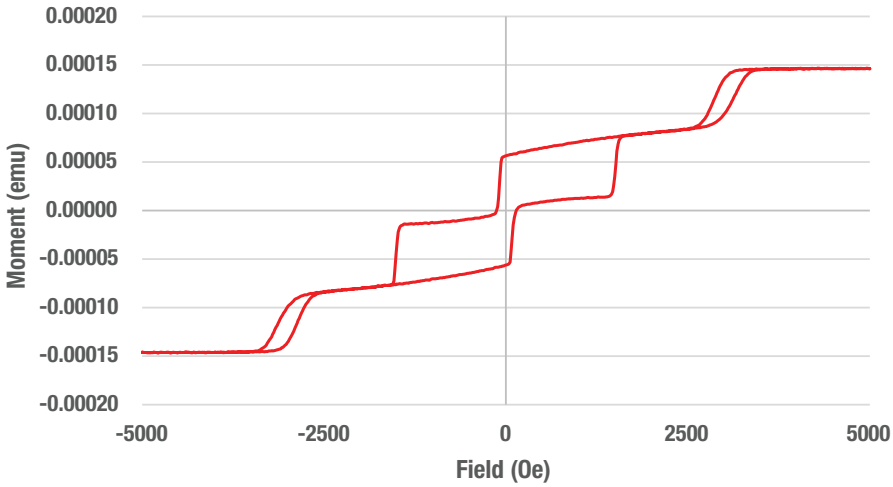

MAGNETIC MULTILAYER

Figure 4

Hysteresis loop for a magnetic tunnel multi-junction stack.

Typical Variable Temperature Results

VARIABLE TEMPERATURE

Figure 1

Hysteresis loops at 100, 200 and 300 K (SSVT) for a core Fe_3O_4 (10 nm)/shell CoO (3 nm) exchange-coupled permanent magnet. There is currently tremendous interest in developing soft (low coercivity)/hard (high coercivity) exchange-coupled magnets as they have the potential to reduce, and potentially eliminate rare-earth constituents that are used in rare-earth magnets (NdFeB, SmCo).

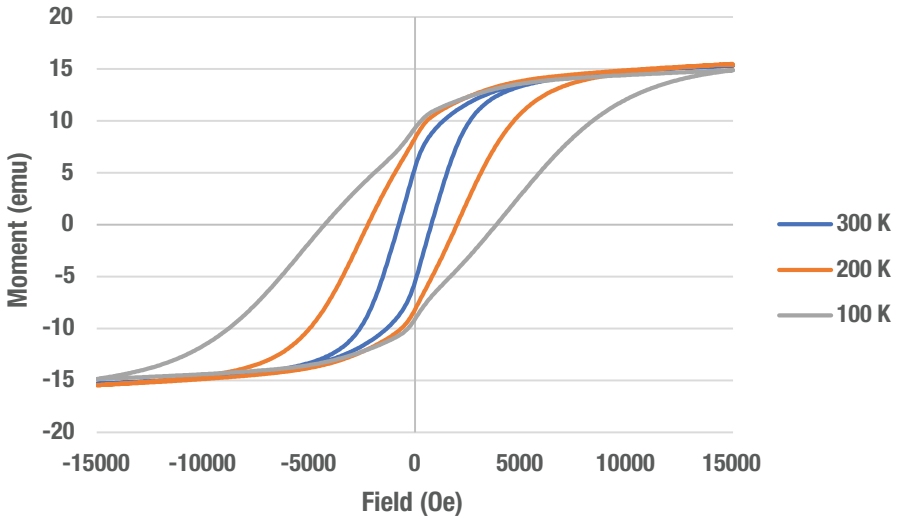

VARIABLE TEMPERATURE

Figure 2

Hysteresis loops at 300, 375, 450 and 525 K (SSVT) for Fe-doped (2%) MnCo nanoparticles (NPs). Doped magnetic nanoparticles (DMNP) are a new class of ferromagnetic nanomaterials that are being studied.

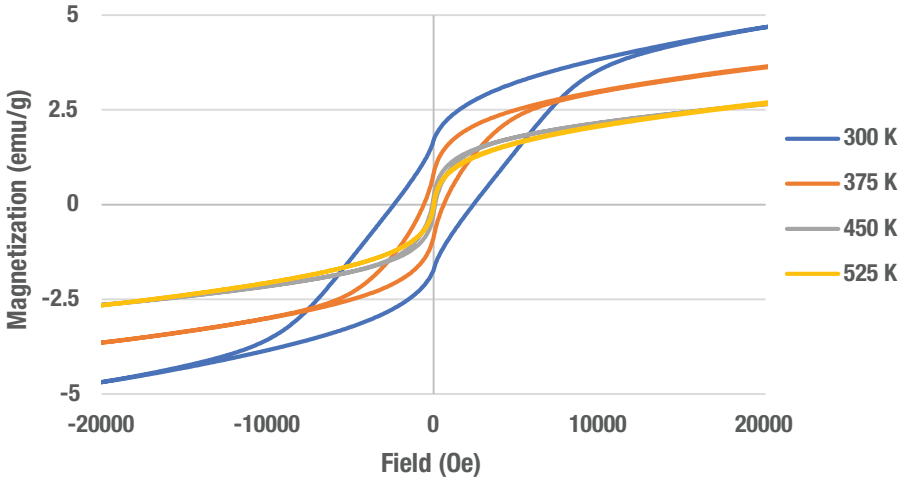

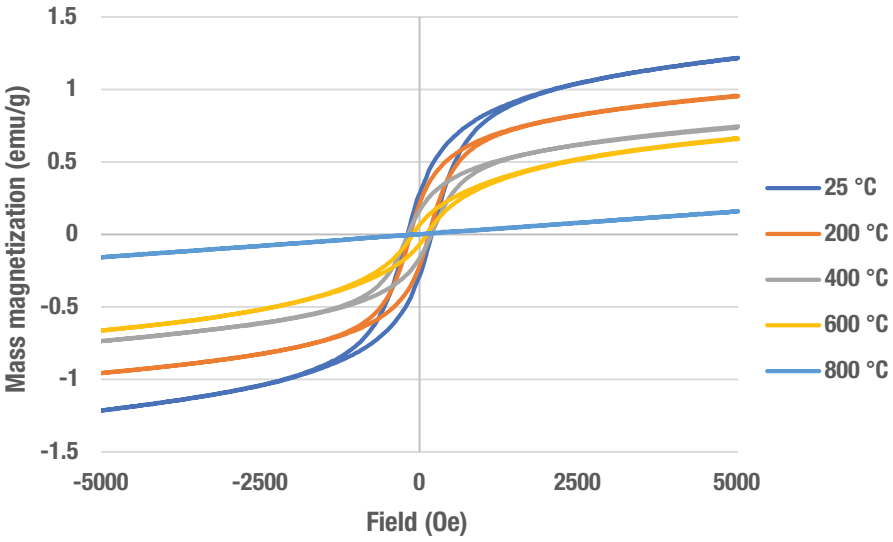

VARIABLE TEMPERATURE

Figure 3

High temperature (oven) hysteresis loops at 25, 200, 400, 600 and 800 °C for Fe-doped (0.5%) MnCo nanoparticles (NPs). As the temperature increases the saturation magnetization (M_s), remanence (M_r) and coercivity (H_c) decrease. The temperature at which a magnetic material transitions from a ferromagnetic (FM) to a paramagnetic (PM) state is called the Curie temperature T_{Curie}, this material is paramagnetic at 800 °C, which is $>T_{Curie}$.

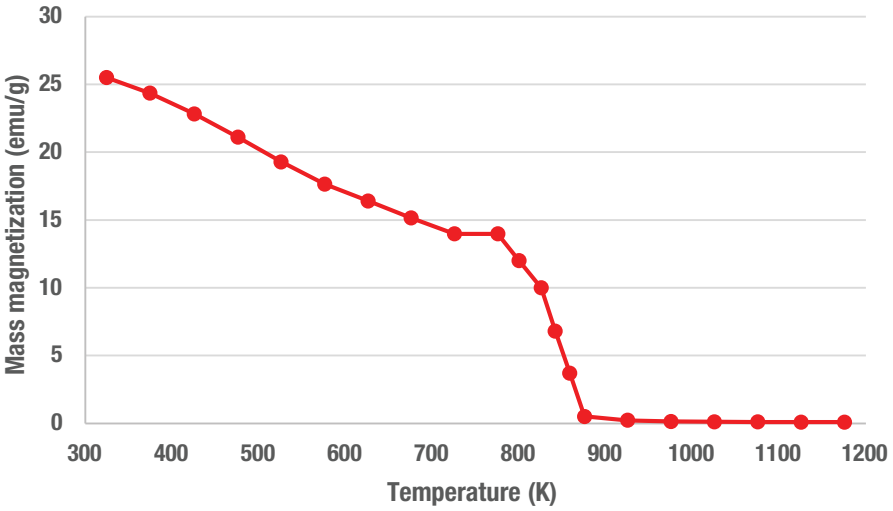

VARIABLE TEMPERATURE

Figure 4

High temperature (oven) $M_s(T)$ for Fe-doped (1%) MnCo nanoparticles (NPs). T_{Curie} for this material is ~925 °C

VARIABLE TEMPERATURE

Figure 5

Low temperature zero-field-cooled (ZFC)/field-cooled (FC) curves for the Fe_3O_4 core (10 nm)/CoO shell (3 nm) nanoparticles (NPs) shown in figure 1. The peak in the ZFC curve at each applied field corresponds to the Blocking temperature T_B. In the 8600 SSVT option with 705 gas controller and 336 temperature controller, measurements of this type are fully automated from low (80 K) to high (950 K), and high to low temperatures.

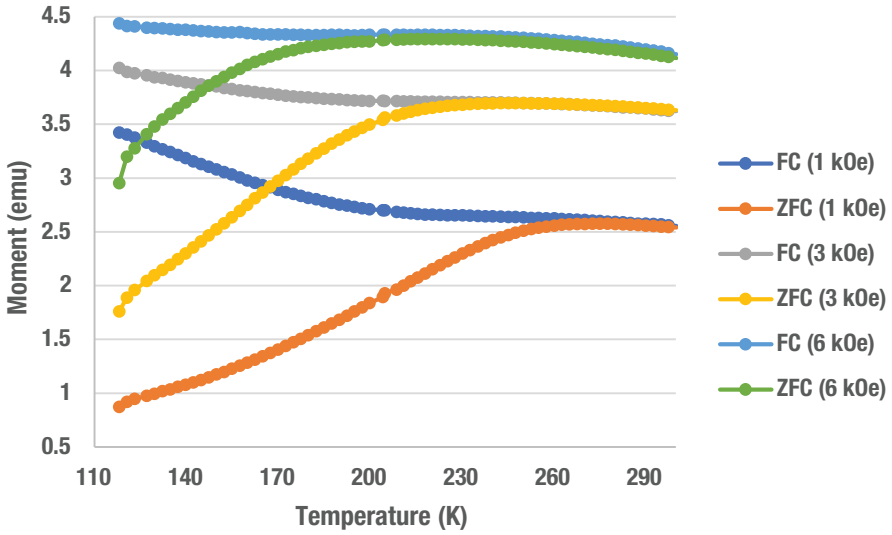

VARIABLE TEMPERATURE

Figure 6

FORC (N = 60) at 120 K (SSVT) for a barium-hexaferrite nanoparticle (NP) soft/hard exchange-coupled permanent magnet. Exchange-coupled magnets can reduce, and potentially eliminate rare-earth constituents that are used in rare-earth magnets (NdFeB, SmCo).

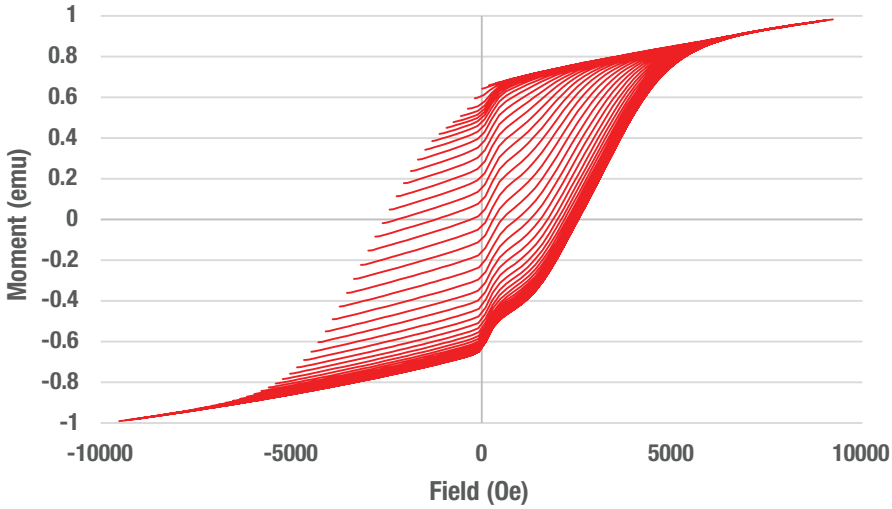

VARIABLE TEMPERATURE

Figure 7

Hysteresis loop at 100 K (SSVT) for a 20 µemu CoPt thin film. This shows that in the SSVT it is possible to measure very low moment samples with good signal-to-noise.

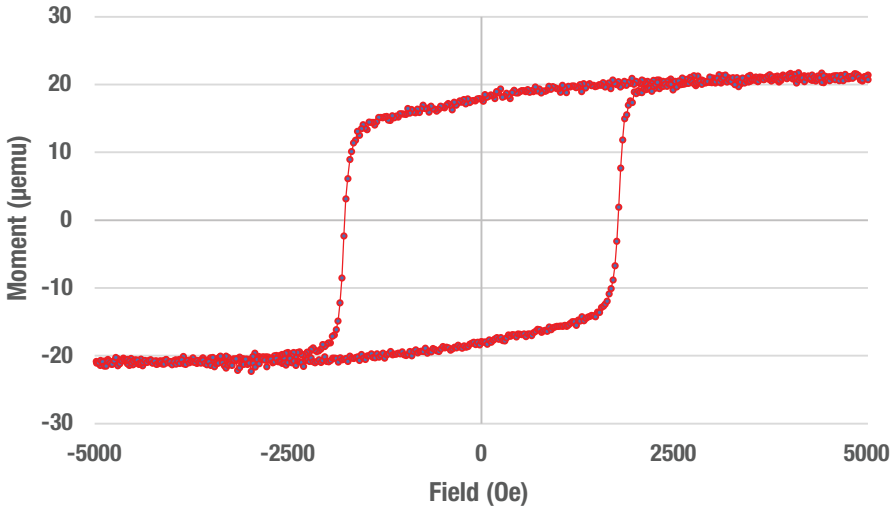

Typical Rotation and Vector Measurement Results

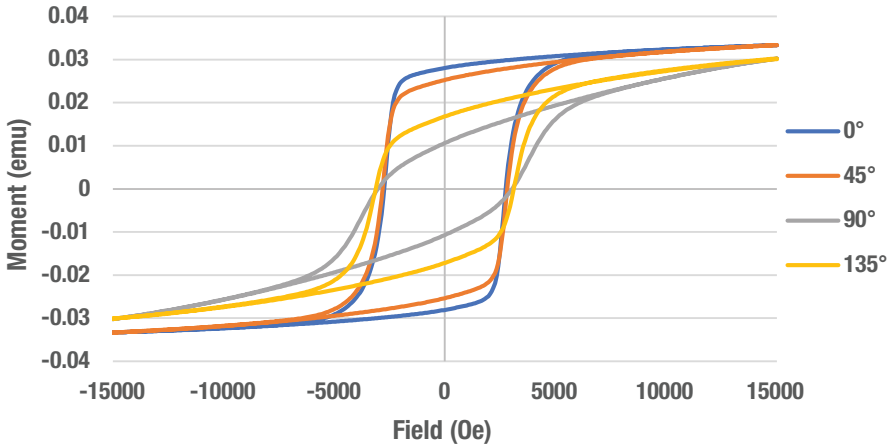

ROTATION AND VECTOR

Figure 1

$M_x(H)$ versus angle for a magnetic stripe.

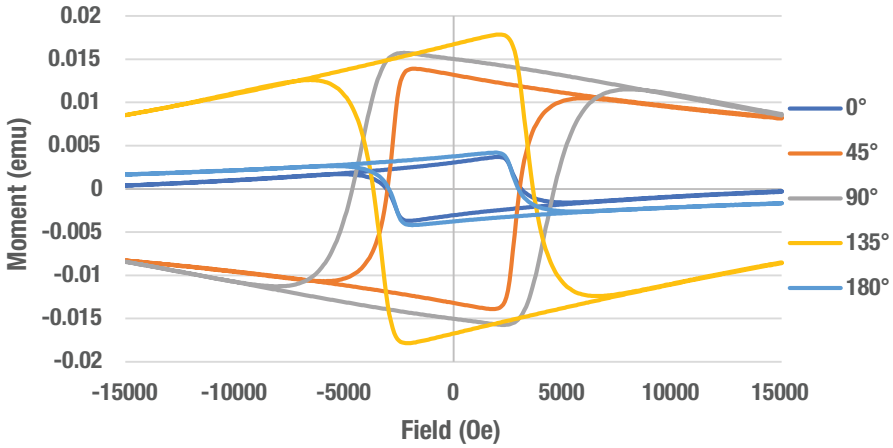

ROTATION AND VECTOR

Figure 2

$M_y(H)$ versus angle for the magnetic stripe shown in figure 1. The $M_x(H)$ and $M_y(H)$ loops at each angle are recorded simultaneously, and the angle is varied automatically (autorotation).

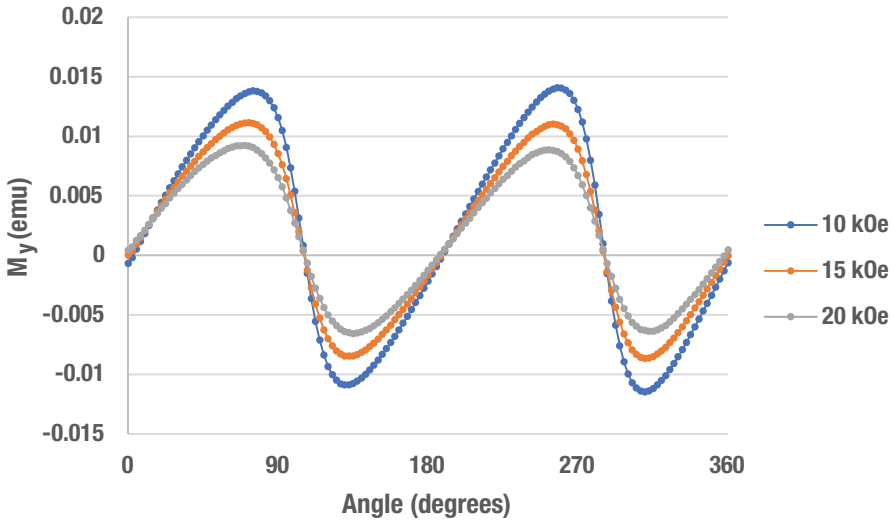

ROTATION AND VECTOR

Figure 3

$M_y(\theta)$ versus applied field for a magnetic stripe exhibiting 2-fold anisotropy. This type of data can be used to derive the torque curve and anisotropy constant of an anisotropic material because the torque density in dyne-cm is: $\tau(\theta) = M_y(\theta)H_x$.

ROTATION AND VECTOR

Figure 4

$M_y(\theta)$ at 20 kOe for a magnetic stripe exhibiting rotational hysteresis. In a rotational hysteresis measurement the angle is swept from 0° to 360° to 0° under full automation (autorotation).

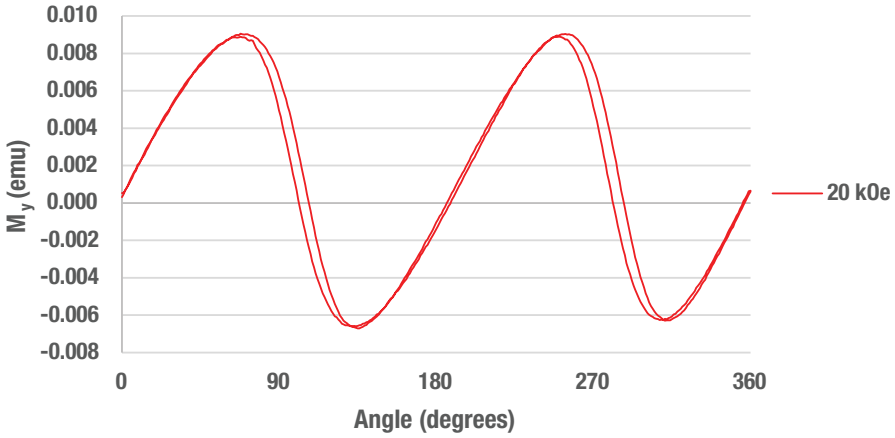

ROTATION AND VECTOR

Figure 5

$M_x(H)$ and $M_y(H)$ for a CoPt thin film. Note that M_y <10 µemu and thus demonstrates the sensitivity of the 8600 y-vector coils.

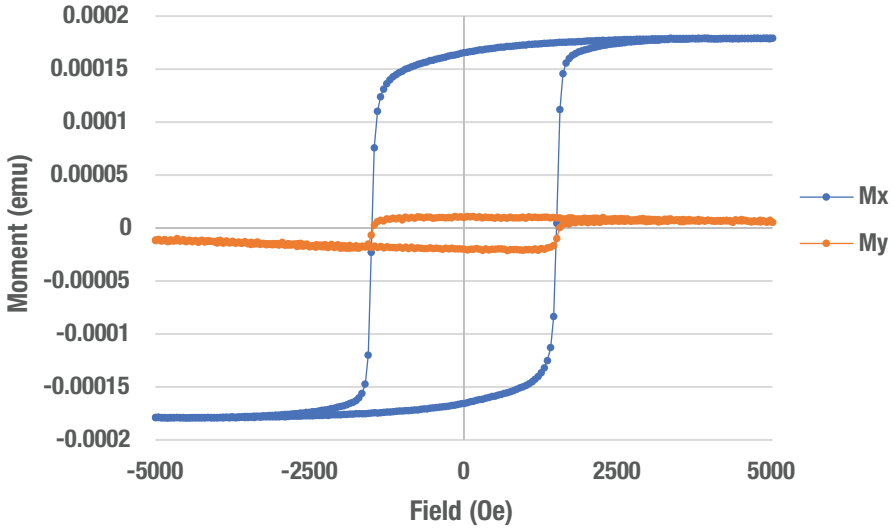

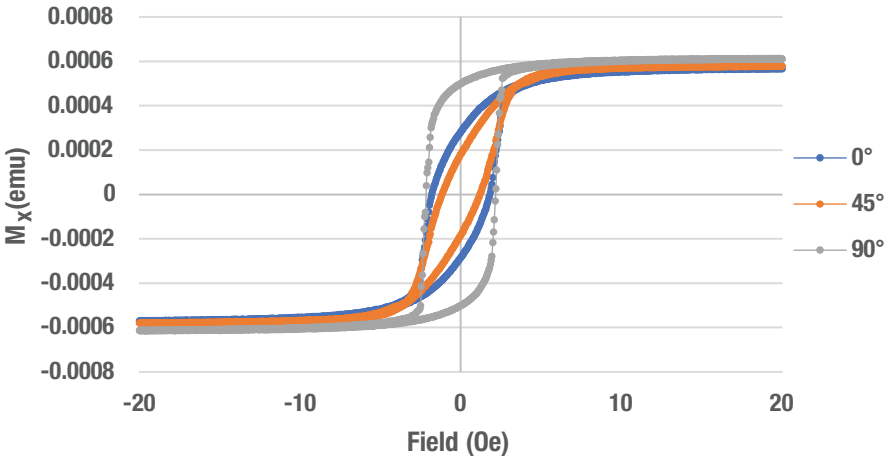

ROTATION AND VECTOR

Figure 6

$M_x(H)$ versus angle for a low coercivity sputtered NiFe thin film.

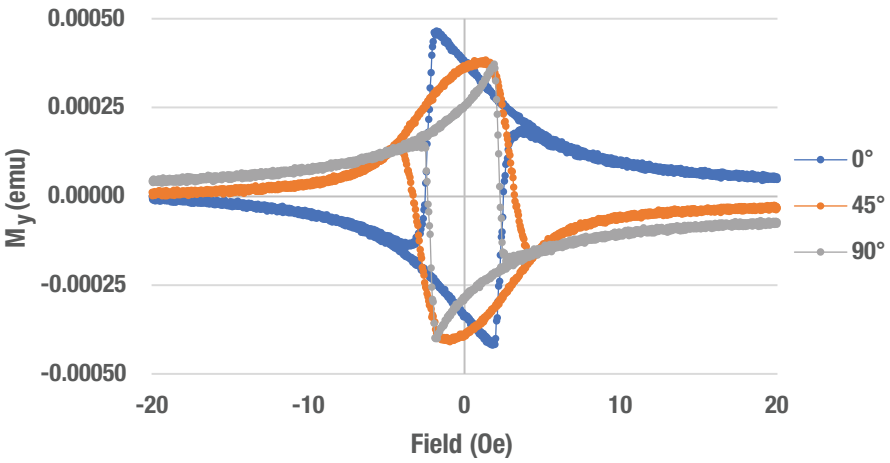

ROTATION AND VECTOR

Figure 7

$M_y(H)$ versus angle for the same low coercivity sputtered NiFe thin film shown in figure 6.

Typical Minor Loop Measurement Results

MINOR LOOP

Figure 1

Descending minor loops (N = 75) for a magnetic stripe. Minor loops probe reversible versus irreversible magnetic processes in materials.

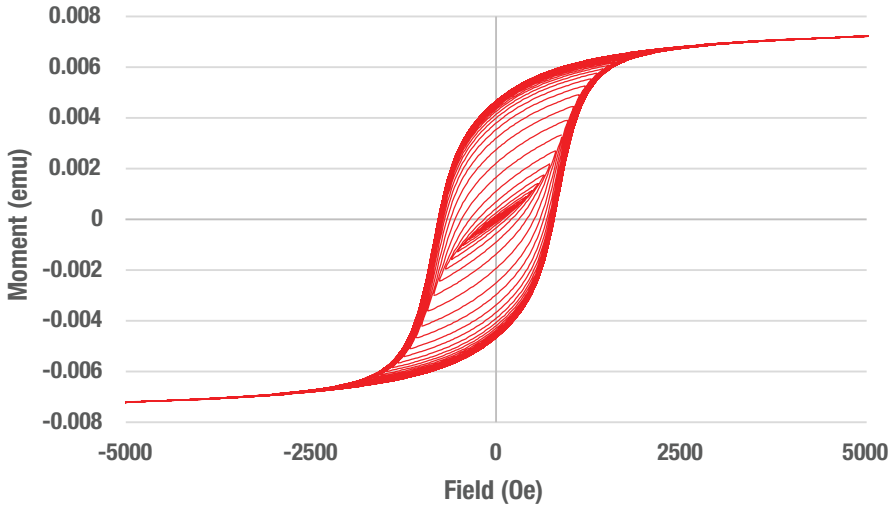

MINOR LOOP

Figure 2

Low moment (30 µemu) ascending minor loops (N = 12) for a CoPt thin film. This data shows that minor loop measurements for low moment samples with high signal-to-noise are possible using the 8600 VSM.

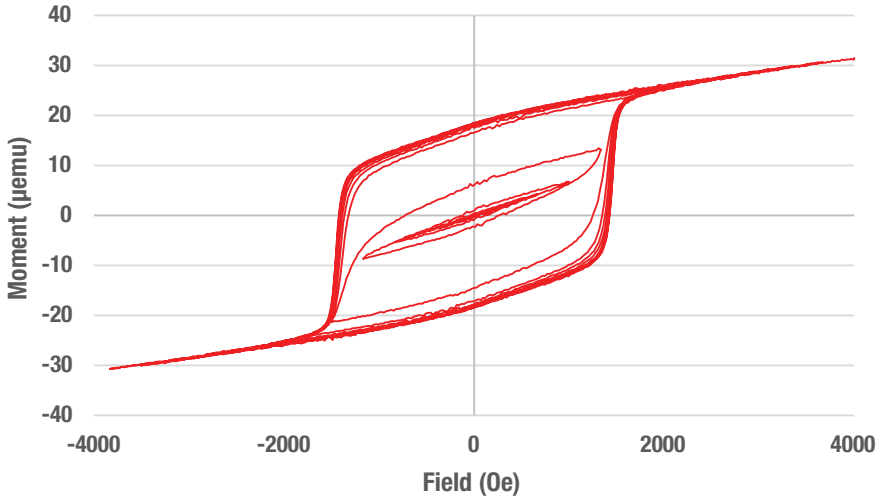

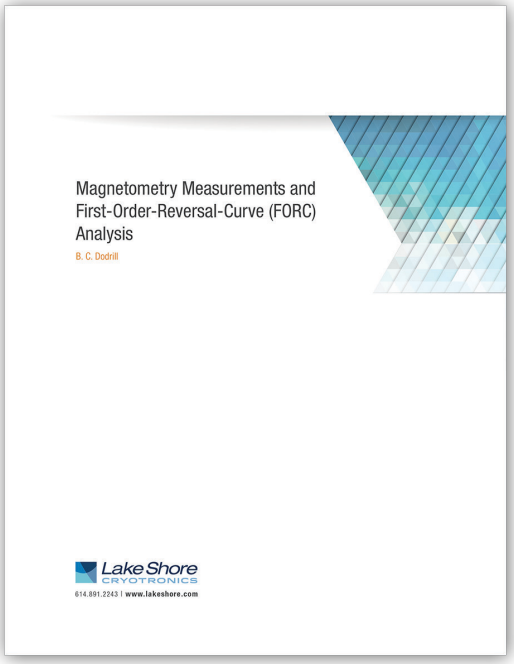

Learn more about FORC. Get our new ebook.

First-order-reversal-curve (FORC) measurements provide far more information than a simple hysteresis loop. They have become indispensable for characterizing interactions and coercivity distributions in a wide array of magnetic materials.

To explore how this elegant material measurement and characterization tool can benefit your magnetics research, submit your info and receive our new, 36-page ebook today.

The ebook discusses FORC theory and presents measurement results for:

- Nanoparticle-based nanocomposites
- Permanent magnets
- Multi-phase ferrite magnets
- Various other materials

Go to www.lakeshore.com/FORC to download the ebook

Send us your sample!

Senior Scientist Brad Dodrill will test your materials on our new 8600 Series VSM and send you the results.

See for yourself how sensitive (15 nemu RMS noise floor) and fast (10 ms/pt) the 8600 Series vibrating sample magnetometers are.

Go to **www.lakeshorecryotronics.com/8600-sample-measurement-request** and Brad will contact you about your samples and give you instructions on how to send them to him.

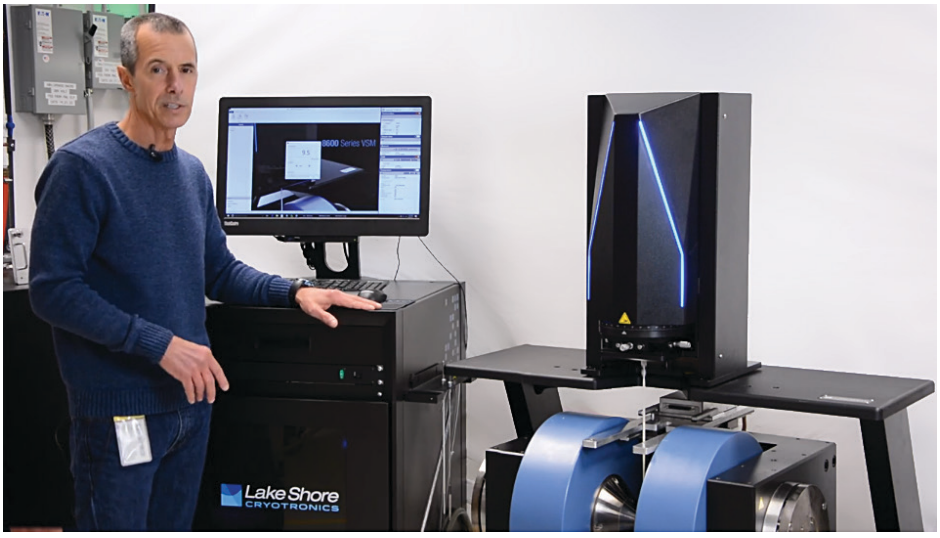

About the author

Brad C. Dodrill is a Senior Scientist at Lake Shore. He graduated from The Ohio State University in 1982 with a BSc degree in Physics and a minor in Mathematics. He completed 2 years of graduate studies in Physics and Electrical Engineering and took a position with Lake Shore Cryotronics in 1984 as a Research Scientist.

In his technical capacity, he is active in applications and product development initiatives in the areas of magnetic and electronic measurements and materials. He has 43 paper publications to his credit, holds 3 U.S. patents, and has lectured at numerous universities and technical conferences in the U.S., Europe, and Asia.

About Lake Shore Cryotronics, Inc.

Supporting advanced research since 1968, Lake Shore (http://www.lakeshore.com) is a leading innovator in measurement and control solutions for materials characterization under extreme temperature and magnetic field conditions. High-performance product solutions from Lake Shore include cryogenic temperature sensors and instrumentation, magnetic test and measurement instruments, probe stations, and precision materials characterizations systems that explore the electronic and magnetic properties of next-generation materials. Lake Shore serves an international base of research customers at leading university, government, aerospace, and commercial research institutions and is supported by a global network of sales and service facilities.